

# Analysis of Ship Groundings on Soft Sea Beds

B. Cerup Simonsen, P. Terndrup Pedersen

Department of Naval Architecture and Offshore Engineering, Technical University of Denmark, Lyngby, Denmark

## Abstract

The consequences associated with ships running aground depend very much on the soil characteristics of the sea bed and the geometrical shape of the ship bow. The penetration into the sea bed depends on these factors and the penetration is an important factor for the ship motion because it influences the ship heave and pitch motions as well as the friction between the ship and the soil.

In this paper a rational calculation model is presented for the sea bed soil reaction forces on the ship bottom. The model is based on the assumption that the penetration of the ship bow generates a flow of pore water through the grain skeleton of the soil. The flow is governed by Darcy's law and it is driven by the pressure of the pore water at the bow. In addition to this pore water pressure, the bow is subjected to the effective stresses in the grain skeleton at the bow surface. These stresses are determined by the theory of frictional soils in rupture. Frictional stresses on the bow surface are assumed to be related to the normal pressure by a simple Coulumb relation. The total soil reaction as a function of velocity and penetration is found by integration of normal pressure and frictional stresses over the surface of the bow.

The analysis procedure is implemented in a computer program for time domain rigid body analysis of ships running aground and it is verified in the paper through a comparison of calculated stopping lengths, effective coefficients of friction, and sea bed penetrations with corresponding experimental results obtained by model tests as well as large-scale tests.

## 1. Introduction

During the last few years much attention has been devoted to accidents where grounding of large tankers resulted in severe oil spills. In [1] and [15] reviews are presented of the recent literature on analysis of ship collisions and ships running aground. The purpose of the present paper is to contribute to the development of a rational analysis procedure for ships running aground on relatively plane, sloping, soft bottoms.

A simplified model for grounding on relatively hard, plane sea beds is presented in Ref. [2] with the emphasis on evaluation of the overall forces induced on the hull girder. In this analysis the model of the grounding event is based on an assumed effective coefficient of friction. The analysis is divided into two phases. In the first phase the ship is subjected to an impulse caused by the sudden contact with the ground. This sudden impact is assumed to be completely unelastic and since the ship is assumed to be stiff the impulse leads to a rapid change of the initial forward

speed so that the ship, after the impact, has a set of surge, heave, and pitch velocity components which are compatible with the motion of the contact point along the sloping bottom. The impulse analysis, presented in Ref. [2], of the first phase of the grounding event can only give rational expressions for the change in momentum and the loss in kinetic energy. It cannot reveal details such as the time variation of the ground reaction forces. For such detailed information it is necessary to have a mathematical model for the interaction forces between the ship bow and the sea bed as the one described in the present paper.

The second phase, considered in Ref. [2], is sliding of the ship bow with continuous contact with the sea bed. The kinetic energy which is available after the end of the first phase is in this second phase transformed into potential energy and into friction between the ground and the ship as the ship moves up on the sloping bottom. In Ref. [2] the forces exerted on the ship bow are assumed to be governed by an effective Coulomb friction law with a constant friction coefficient which can only be determined by experiments. This is due to the fact that, besides the ordinary friction between steel and ground, the effective coefficient of friction includes pressure forces on the bow perpendicular to the motion due to penetration of the bow into the sea bed. Therefore, in order to obtain a better basis for analysis of ships running aground on soft grounds, there is a need for a mathematical model for the interaction between ship and ground which can be used in a consistent way to determine the detailed behaviour during the initial phases of the contact with the ground and, at the same time, to calculate the effective coefficient of friction in the second phase of the grounding event. The grounding forces on a ship bow arise when the bow is being pressed into the saturated soil. This generates a movement of the soil and of the pore water. In general, the dynamic behaviour of saturated soil is strongly influenced by the presence of pore water, and the phenomenon of large dynamic deformations of saturated soil is extremely difficult to model numerically. In the present analysis, it is assumed that the penetration of the ship bow generates a flow of pore water through the grain skeleton. This flow is governed by Darcy's law and it is driven by the pressure in the pore water at the bow. In addition to this pore water pressure, the bow is subjected to the effective stresses in the grain skeleton at the bow surfaces. These stresses are determined by the theory of frictional soils in rupture. Frictional stresses on the bow surface are assumed to be related to the normal pressure by a simple Coulomb relation. The total soil reaction force is found by integration of normal pressure and frictional stresses over the surface of the bow. Due to the special form of ship bows, the contact area between soil and bow can be approximated by a series of ellipsoidal forms and planes. This is used in the calculation of the soil and pore water kinematics. The analysis procedure is implemented in a time domain computer program for rigid ships running aground and it has been verified through a comparison of calculated stopping lengths, effective coefficients of friction, and sea bed penetrations with corresponding experimental results obtained by model tests as well as full-scale tests. In subsequent papers [3], [15] and [16], the effect of hull flexibility and hydrodynamic memory effects on the transient hull motions are analyzed.

## **2. The Soil Mechanics Model**

### **2.1 Dynamic Loading of Saturated Soils**

It is well known, see Mei, Yeung, and Liu [4], that the behaviour of soils is strongly influenced by the pressure of fluid present in the pores of the material. This fact can be experienced at the beach. When one runs in the submerged sand close to the waterline the sand feels hard whereas the dry sand feels very soft in comparison. In traditional soil rupture theory [5], conditions are assumed to be either drained or undrained. If conditions are drained an extra load on a soil element is carried solely by additional stresses in the grain skeleton ("effective stresses"), and if con-

ditions are undrained an extra load is carried by an additional pressure in the pore fluid alone. Both drained and undrained conditions are considered independent of the time history of the load and in this case of the impact velocity - and neither of these classical theories are therefore suited for modelling of ship grounding events. In consolidation theory the time variance of loads and deformations is considered. Biot, [6], [7], presented a general set of equations governing the behavior of a saturated linear elastic porous solid under dynamic conditions. For standard geotechnical problems, the grain skeleton is most often assumed to be linear and elastic and inertia forces are neglected.

Biot's equations can be generalized to non-linear material behaviour if the constitutive relation is written incrementally. A fully consistent theoretical analysis of a ship grounding event would require solution of these equations for example by use of the finite element method. The solution would include phenomena like elastic compression, rupture with very large plastic strains, liquefaction, dilatation of the soil in rupture, and flow of pore water. Use of such a model for grounding simulations will require extensive computer facilities and it will be very time-consuming. Therefore, the soil mechanics model used here has been based on very substantial simplifications and it is to some extent phenomenological. The model experiments briefly mentioned in Ref. [2] suggest that when the ship velocity is relatively high, the soil reaction is governed by pressure in the pore fluid. On the other hand, for very small ship velocities (for example after the ship has stopped) conditions are drained and the soil reaction is therefore the result of the effective stresses in the grain skeleton alone.

The model used in the present analysis is based on the assumption that the soil reaction can be found as the sum of two contributions, see Ref. [13]:

1. A force from the pressure in the pore water around the bow. It is assumed that pore water is pressed into the grain skeleton, corresponding to the motion of the bow and that velocities of sand grains can be neglected (i.e. generally small compared to that of the pore water).
2. A force corresponding to a drained rupture around the bow.

This model is expected to give good results in the following two cases:

1. High velocity and elastic compressible of the grain skeleton. This case corresponds quite well to ships with bulbous bows grounding with high velocity on soils with small permeability.
2. Drained conditions and fully developed rupture conditions in the soil that carries the bow. This case corresponds to both bulbous bows and V-shaped bows in highly permeable material at low speeds or to the period after the ship has stopped.

In other cases, this model cannot be expected to predict soil forces with the same accuracy because the displacement of the grains is not small compared to that of the pore water; the pore water is not pressed through a steady grain skeleton.

The frictional stress on the bow is assumed to be a constant fraction of the normal pressure. In the following section it is shown how the two contributions to the force from the normal pressure is calculated.

## **2.2 Force from Pore Water Pressure**

Equilibrium of the fluid phase in saturated soil can be expressed as ([7], [9])

$$-p_i = \frac{\rho_w(1+e)}{e} \ddot{v}_i + \rho_w g \left( \frac{1}{k} + b\dot{w}_i \right) \dot{w}_i \quad (1)$$

where,

- $b$  : empirical constant accounting for non-linearities in Darcy's law at high flow velocities,
- $g$  : acceleration of gravity,
- $\cdot_i$  : the spatial derivative with respect to the  $i$ 'th component,
- $k$  : permeability coefficient for laminar flow (Darcy's law),
- $p$  : pore pressure (above hydrostatic pressure),
- $u_i$  : absolute displacement of solid phase,
- $v_i$  : absolute average displacement of fluid phase,  $\dot{v}_i$   
: is absolutely filter velocity,i.e. appropriate volume rate divided by total area,
- $w_i$  : average pore water displacement relative to solid phase  $w_i = v_i - u_i$
- $\dot{w}_i$  : relative filter velocity, i.e. appropriate volume rate divided by total area,
- $\rho$  : density of water

The term  $b\dot{w}_i$  was introduced by Engelund, [9], to account for non-linearities in Darcy's law at high flow velocities. In [9] it is shown that the linear permeability coefficient can be calculated as

$$k = \frac{e^2(1+e)}{\alpha} \frac{gd^2}{\nu_w} \quad (2)$$

and the correction factor,  $b$ , as

$$b = \beta \frac{(1+e)^2}{e^3} \frac{1}{gd} \quad (3)$$

in which

- $d$  : mean diameter of grains,
- $e$  : void ratio, i.e. pore volume/grain volume, and
- $\nu_w$  : kinematic viscosity of water

$$(\alpha, \beta) = \begin{cases} (800, 1.8) : \text{for spherical equal-sized grains.} \\ (1000, 2.8) : \text{for uniform, round grains} \\ (1500, 3.6) : \text{for irregular, edged grains} \end{cases} \quad (4)$$

For a stationary flow of pore water with moderate flow velocities, Eq. (1) reduces to the usual form of Darcy's law:

$$-p_{,i} = \frac{\rho_w g}{k} \dot{w}_i \quad (5)$$

Eq. (1) can be linearized by introducing an effective permeability coefficient,  $k_e$ , defined by

$$\frac{1}{k_e} = \frac{1}{k} + b \cdot |\dot{w}_a| \quad (6)$$

where  $|\dot{w}_a|$  is an average relative flow velocity.

In the following, it is assumed that the displacement of the grain skeleton is small compared to that of the pore water. Then  $w_i = v_i$  and Eq. (1) becomes

$$-p_{,i} = \frac{\rho_w(1+e)}{e} \dot{v}_i + \frac{\rho_w g}{k_e} \dot{v}_i \quad (7)$$

Application of the continuity condition,  $v_{i,i} = 0$ , to Eq. (7) yields the Laplace equation:

$$\nabla^2 p = \frac{\partial^2 p}{\partial x^2} + \frac{\partial^2 p}{\partial y^2} + \frac{\partial^2 p}{\partial z^2} = 0 \quad (8)$$

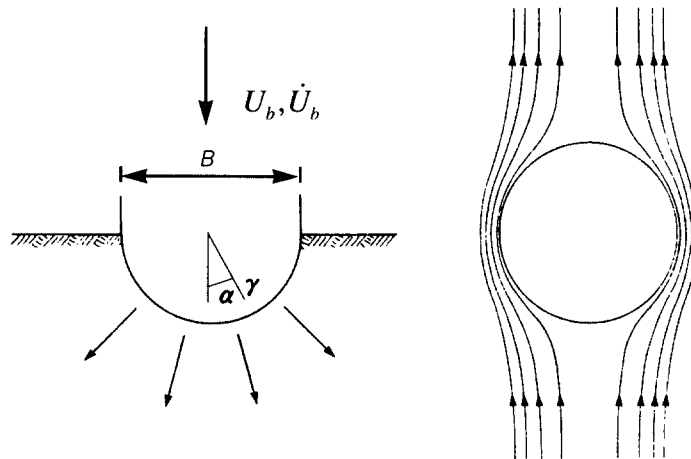


**Figure 1.** Pore water flow around a section of the bow

To illustrate how the total pore water pressure on a bow is calculated, we may consider the example shown in Figure 1.

A plane problem is considered but the method is the same for a three-dimensional problem. A semi-circular body is pressed with velocity  $\dot{U}_b$  and acceleration  $\ddot{U}_b$  into a saturated soil. The boundary conditions are

- No fluid flow into the bow.
- The pressure is zero at the soil surface

Several solutions to Laplace's equation, Eq. (8), are known for different geometrical forms and boundary conditions (e.g. [10], [11]). In [10] the motion of a rigid body in an ideal fluid, as illustrated in Fig. 1, is considered. This problem is also governed by Eq. (8). The solution is given in [10] in terms of a pressure potential,  $\varphi$ .

Expressed as a function of a radial coordinate,  $r$  and an angular coordinate  $\alpha$ , see Figure 1, the pressure on the bow is

$$p(r, \alpha) = \frac{1}{4} \frac{B^2 \cos \alpha}{r} \kappa \quad (9)$$

where,

$$\kappa = \frac{\rho_w(1+e)}{e} \ddot{U}_b + \frac{\rho_w g}{k_e} \dot{U}_b \quad (10)$$

Integrating  $p$  from Eq. (9) over the surface of the bow would give the total force exerted by the pore water pressure.

In the case of a rigid body accelerated in an ideal fluid, the result of the fluid pressure,  $F_R$ , is conveniently expressed in terms of added-mass or inertia coefficients, often as

$$F_R = \rho_w C_m V_R a \quad (11)$$

where

$a$  : acceleration,

$C_m$  : added-mass coefficient,

$V_R$  : volume of reference, often equal to the displaced volume

In the example of a circular body with diameter  $B$ ,  $C_m = 1$  and  $V_R = \frac{\pi}{4} B^2$ . Due to the aforementioned analogy, knowledge of the added mass of a given problem can similarly be applied to a drainage problem. In the example shown in Fig. 1 the total force from the pore water can be calculated as

$$F_p = \frac{1}{2} C_m V_R \kappa \quad (12)$$

where the factor of 1/2 being necessary because  $C_m V_R$  is calculated for a completely immersed body subjected to fluid pressure on all sides.

Added-mass characteristics,  $C_m V_R$ , are tabulated for a large number of geometries and boundary conditions. Therefore, Eq. (12) represents a very convenient form of calculation of the result of the pore water pressure in a numerical scheme.

### 2.3 Force Corresponding to Drained Rupture

During grounding in normal sand, the force from the pore water will be dominating during most of the time. Only at very low velocities and when it has stopped, the soil reaction will be governed by the drained soil reaction.

Rupture around the bow is clearly three-dimensional but the assumption of plane stress is adopted with a subsequent correction for the three-dimensionality of the problem. The sides of the ship, the bulb, and the ship bottom are considered separately. The part of the bulb in contact with the soil is approximated by a plane surface so that only plane surfaces are considered. With these assumptions, standard formulae for drained rupture in saturated sand can be used.

If it is assumed that the rupture is fully developed and that strain hardening can be ignored, the normal effective soil pressure on the sides can be calculated by use of the theory for passive soil pressure on plane walls. The soil pressure,  $e_s$ , normal for the wall in the depth  $d_p$  is

$$e_s = \gamma' d_p K_\gamma \quad (13)$$

where  $\gamma'$  is the submerged weight of the soil, and the rupture coefficient  $K_\gamma$  is a function of frictional angle, slope inclination, and surface roughness as it is given in standard geotechnical literature(e.g. [5]).

Eq. (13) can be integrated to give the normal force on the ship sides.

The maximum possible soil reaction on the ship bottom is found from the theory of load capacities of foundations. A strip of  $dl$  and width  $B$  can carry the load

$$dQ = \frac{1}{2} \gamma' N_\gamma B^2 dl \quad (14)$$

where the coefficient  $N_\gamma$  is given in standard geotechnical literature(e.g. [5]). Integration of Eq. (14) along the length of the contact area gives the load capacity,  $Q$ , based on the assumption of two-dimensional rupture. To compensate for three-dimensional effects,  $Q$  is reduced by an empirical factor of  $s_\gamma = (1 - 0.4 B_{max}/L_{max})$  where  $B_{max}$  and  $L_{max}$  are, respectively, maximum width and maximum length of the contact area ( $B_{max}/L_{max} < 1$ ).

This maximum load,  $Q_{max} = s_\gamma \cdot Q$ , is not necessarily reached over the whole contact area of the ship bottom - in some areas the ground will be elastically compressed and in some areas the rupture is fully developed. Therefore, the loading and unloading behaviour up to and from the

maximum load has to be defined. This is particularly important in the final phase where equilibrium between the hydrostatic forces on the ship hull and the soil reaction on the bottom has to be reached. From tests with passive soil pressure on the plane walls it is known that the maximum soil pressure is mobilized after a displacement of approximately 1-5 percent of the height of the wall. It is here assumed that the load,  $Q_{max}$ , corresponding to a fully developed rupture, is reached after a compression of a certain fraction  $\delta$  of  $B_{max}$ . Correspondingly, unloading from  $Q_{max}$  is assured to occur over a distance of  $\delta \cdot B_{max}$ . Fortunately the grounding behaviour and final resting position turn out to be quite insensitive to the choice of  $\delta$  so that a fixed value of  $\delta = 0.03$  is used.

### 3. Analysis Model & The Rigid Hull Motion

#### 3.1 Geometry and Coordinate Systems

The grounding behaviour is quite sensitive to the bow geometry and the numerical model must therefore include a reasonable representation of the actual geometry. Many bulbous bows have the shape of a half-sphere mounted on a cylinder, and this is easily represented mathematically. The rest of the bow often consists of double curved surfaces. Such general shapes cannot be defined by simple analytical functions. In the present numerical model the idealization shown in Fig.2 is used. The soil pressure on a V-bow is assumed to work on the ship bottom and on the plane sides defined by the points A,B, and C in Fig. 2. When a bulbous bow is considered an additional soil reaction on the front spherical part is calculated.

Two coordinate systems are used: A local  $xyz$ -coordinate system which is fixed in the ship

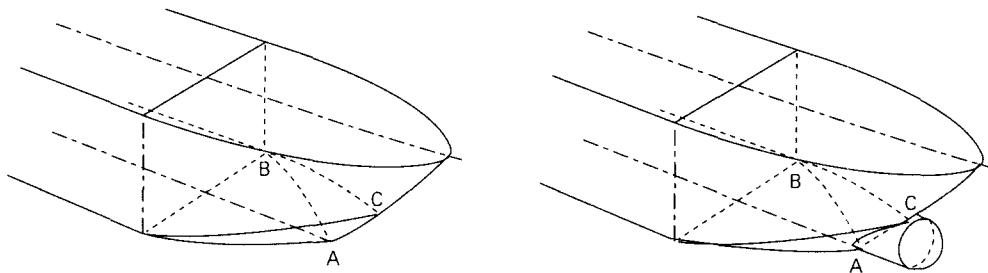


**Figure 2.** Idealization of V-bow bulbous bow used in the calculation model

and a global  $XYZ$ -coordinate system which is fixed in the relation to the sea bottom, see Fig. 3. The local coordinate system has its origin amidships. The  $x$ -axis points forward and coincides with the ship base line. The  $y$ -axis points horizontally towards the port side and the direction of the  $z$ -axis is upwards. The global system has its origin at the point of initial contact. The  $X$ -axis lies horizontally in the plane of symmetry of the ship pointing in its forward direction. The  $Z$ -axis points in the direction opposite to the gravity field and the global  $Y$ -axis points in the same direction as the local  $y$ -axis.

The geometry and the mass distribution are defined in the local coordinate system. The global surge and heave positions of the ship are given by the  $X$  and  $Z$  coordinates of the origin if the local coordinate system. The pitch rotation,  $\theta$ , is defined as the angle between the global  $X$ -axis

and the local  $x$ -axis with the positive direction of rotation being defined by the  $y$ -axis.

As indicated in Fig 3. the ship is assumed to sail with an initial velocity  $V$  perpendicularly onto a sloping sea bed bottom which has a bilinear geometrical form.

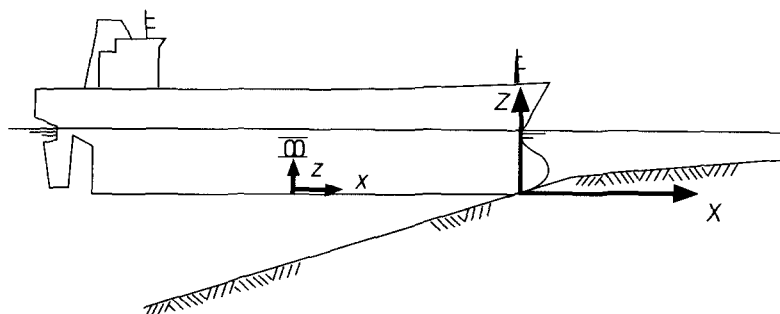


Figure 3. Definition of coordinate system

### 3.2 Equation of Motion

In the present analysis we assume that the ship hull is rigid and the hydrodynamic pressure forces acting on the ship hull during the grounding event can be approximated by constant hydrodynamic added-mass terms. These assumptions are released in subsequent papers [3], [15] and [16]. With these assumptions the equation of motion can be expressed in the following form (see Ref. [12]):

$$\begin{bmatrix} M_{xx} & 0 & z_g M_{xx} \\ 0 & M_{zz} & -x_{gz} M_{zz} \\ z_g M_{xx} & -x_{gz} M_{zz} & J_y \end{bmatrix} \begin{Bmatrix} \ddot{u} \\ \ddot{w} \\ \ddot{\theta} \end{Bmatrix} = \begin{Bmatrix} F_x \\ F_z \\ M_{mom} \end{Bmatrix} + \begin{Bmatrix} M_{zz}(x_{gz}\dot{\theta}^2 - \dot{\theta}\dot{w}) \\ M_{xx}(\dot{\theta}\dot{u} + z_g\dot{\theta}^2) \\ -M_{zz}(z_g\dot{\theta}\dot{w} + x_{gz}\dot{u}\dot{\theta}) + (M_{zz} - M_{xx})\dot{u}\dot{w} \end{Bmatrix} \quad (15)$$

where  $\dot{u}$  is the ship surge velocity in the  $x$ -direction,  $\dot{w}$  the heave velocity at  $x=0$ , and  $\dot{\theta}$  the pitch velocity.

If we denote the added hydrodynamic mass per unit length by  $\mu_x(x)$  and  $\mu_z(x)$  in the  $x$ - and the  $z$ - direction, respectively, the hull mass per unit length by  $m(x)$ , and the mass moment of inertia per unit length by  $j_y(x)$  we have

$$\begin{aligned} M_{xx} &= \int_L \{m(x) + \mu_x(x)\} dx \\ M_{zz} &= \int_L \{m(x) + \mu_z(x)\} dx \\ x_{gz} &= \int_L \{m(x) + \mu_x(x)\} x dx / M_{zz} \\ z_g &= \int_L \{m(x) + \mu_z(x)\} z dx / M_{xx} \\ J_y &= \int_L \{j_y(x) + x^2(m(x) + \mu_z(x))\} dx \end{aligned}$$



This system of equation is solved for the accelerations in the local coordinate system. These may then be transformed to the global system by

$$\begin{aligned}\ddot{X} &= \ddot{u} \cos \theta + \ddot{w} \sin \theta + (-\dot{u} \sin \theta + \dot{w} \sin \theta) \dot{\theta} \\ \ddot{Z} &= -\ddot{u} \sin \theta + \ddot{w} \cos \theta + (-\dot{u} \cos \theta - \dot{w} \sin \theta) \dot{\theta} \\ \ddot{\theta}_y &= \ddot{\theta}\end{aligned}\tag{16}$$

Since we neglect the effect of propeller and rudder forces the only external forces  $\{F_x, F_z, M_{mom}\}^T$  are the sum of the static restoring forces and the soil reaction forces. The derivation of the soil reaction forces was described in Section 2.

The restoring forces are the result of hydrostatic pressure and gravity. On the assumption of linear behaviour, the vertical restoring force,  $\Delta F_z$ , and the restoring moment,  $\Delta M_r$ , given heave,  $\Delta Z$ , and pitch,  $\Delta \theta_y$ , displacements from the equilibrium condition can be calculated as

$$\begin{Bmatrix} \Delta F_z \\ \Delta M_r \end{Bmatrix} = \begin{bmatrix} (\rho_w g A_{wl}) & (-\rho_w g A_{wl} x_F) \\ (-\rho_w g A_{wl} x_F) & (\rho g \nabla \overline{GM}_L + \rho_w g A_{wl} x_F^2) \end{bmatrix} \begin{Bmatrix} -\Delta Z \\ -\Delta \theta_y \end{Bmatrix}\tag{17}$$

where,

- $A_{wl}$  : area of waterline
- $x_F$  : longitudinal position of centre of floatation,
- $\nabla$  : displacement volume,
- $\rho_w$  : density of the displaced water,
- $\overline{GM}_L$  : longitudinal metacentric height

#### 4. Verification and Examples

The model tests briefly described in[2] have been used for verification of the calculation model. A free-floating tanker model with a bulbous bow and length  $L_{pp} = 2.57m$  in scale 1:60 was forced into a sand slope of 1:6 with a constant velocity of 0.464 m/s. The sand had a mean diameter  $d = 0.125 mm$ , permeability coefficient  $k = 8.5 \cdot 10^{-5} m/s$ , and Coulomb frictional angle  $41^\circ$ . Figs. 4-6 show measured and calculated penetrations into the slope, vertical ground reactions, and effective coefficients of friction. The effective coefficient of friction is the ratio between the round reaction perpendicular to the slope and the ground reaction in the direction tangential to the

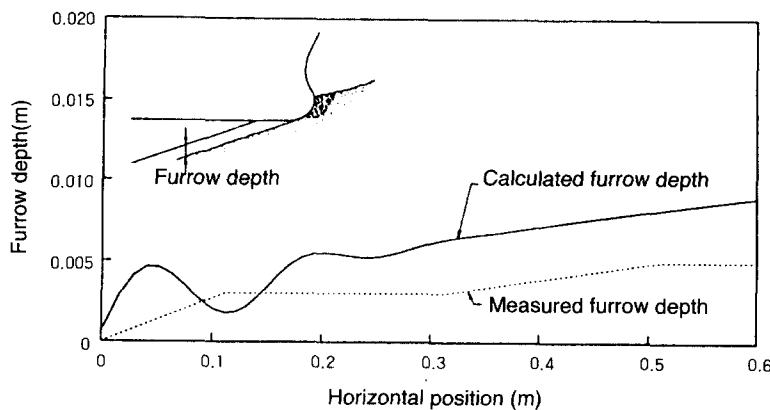


**Figure 4.** Measured and calculated furrow depths

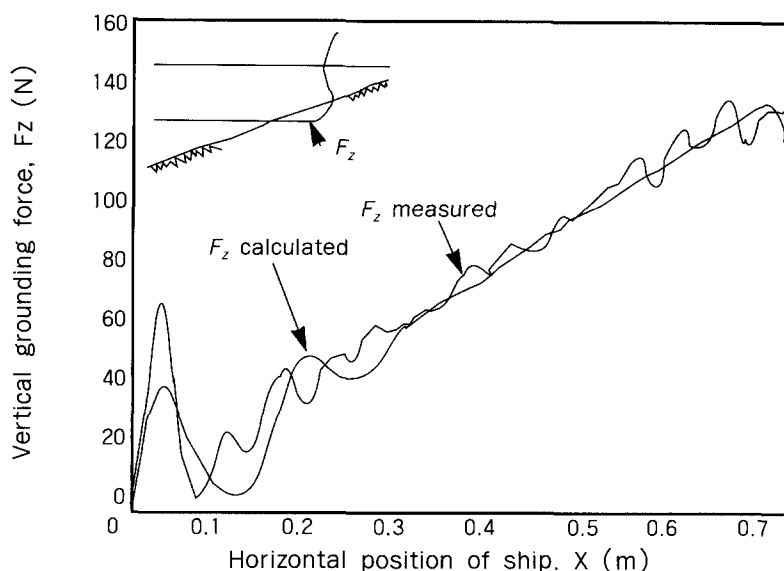


**Figure 5.** Measured and calculated vertical soil reaction

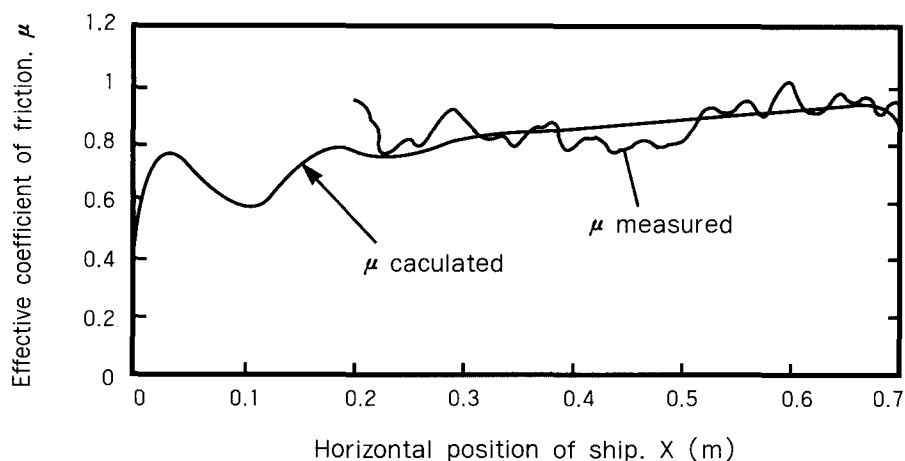


**Figure 6.** Measured and calculated effective coefficient of friction

slope. A good correspondence between measurements and calculations is observed. It is noted that the effective coefficient is significantly greater than the traditional sand/steel Coulomb frictional coefficient which is 0.3 - 0.4.

A number of grounding tests were carried out with a condemned vessel with a V-shaped bow, a displacement of 300 metric tons, a length between perpendiculars of 29.55 m, a moulded breadth of 6.60 m and a draught amidships of 2.67 m, see Ref.[14] The bow consists of highly curved surfaces so when the geometry idealization shown in Fig.2 is used, only the part of the bow that is in contact with the soil is considered. Table 1 shows the measured stopping distances together with corresponding calculated values. Different slope inclinations are considerable in order to take into account the uncertainty of the slope measurements and the actual variation of

slope inclination. Tests 1 and 2 are best suited for verification because they were performed in calm water and the slope measurements were the most accurate. For these tests the calculation model gives too large stopping distances - the maximum deviation is seen to be 21%.

As an application example, grounding of a 220,000 DWT tanker with an initial velocity of 5.1 m.s is considered. The main particulars of the ship are: length,  $L_{pp} = 269.0 \text{ m}$ ; breadth = 36.6 m; draught = 13.2 m; trim = 3.0 m; mass =  $1.07 \cdot 10^8 \text{ kg}$ . A sea bed of coarse sand ( $d = 2 \text{ mm}$ ,  $e = 0.6$ , and frictional angle  $37^\circ$ ) is considered. The inclination of the slope is 1:6 more than 7 m below the water surfaces and 1:20 above this level. The stopping distance is found to be 42.1 m. Fig. 7 shows the track of the bulb compared to the undisturbed sea bed. The maximum penetration is seen to be approximately 1 m and the final bow lift 4.5 m. Fig. 8 shows the vertical component if the ground reaction and the effective coefficient of friction for this grounding event.

**Table 1.** Large-scale test. Measured and calculated stopping distances

Test No.	Measured			Calculated			
	Impact velocity	Slope 1:X	Stopping distance (m)	Slope 1:X	Stopping distance (m)	Slope 1:X	Stopping distance (m)
1	2.5	12-14	9.6	12	10.9	14	11.6
2	5.1	9-11	16.4	9	16.6	11	18.1
3	5.1	4-6	12.1	4	9.9	6	13.4
4	4.1	4-6	8.1	4	8.3	6	11.1
5	4.1	10-15	16.6	10	14.7	15	17.3
6	5.0	8-15	17.3	8	16.7	15	19.8
7	4.5	11-18	13.2	11	17.2	18	20.7

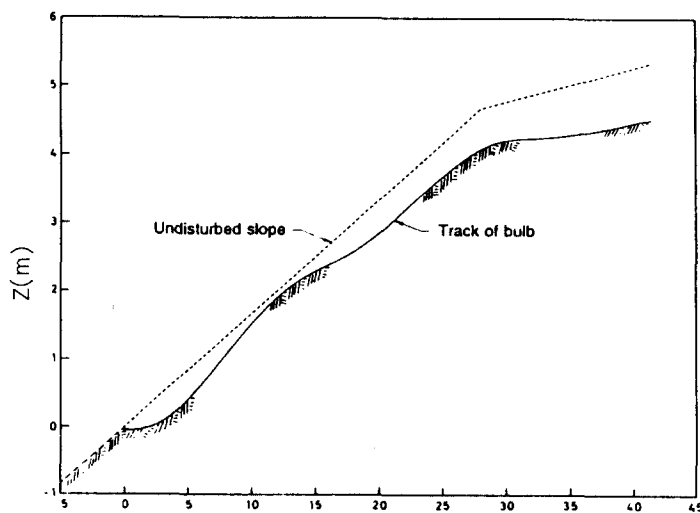


**Figure 7.** Slope and track of bulb during grounding of 220,000 DWT tanker

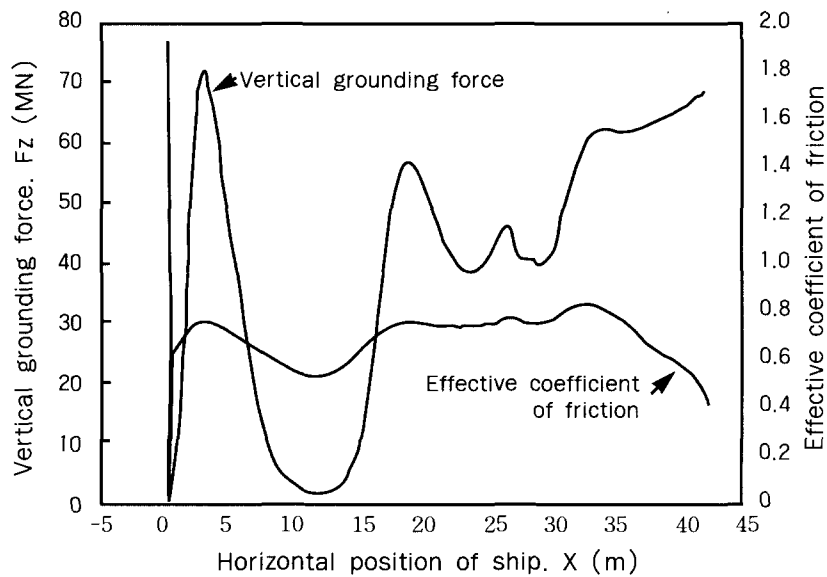


**Figure 8.** Vertical component of ground reaction and effective coefficient of friction

## Conclusion

Prediction of damages due to ship grounding is an important part of marine risk assessment. By presenting a simple, rational analysis procedure for the interaction between the ship hull and the sea bed during grounding, it has been the purpose of this paper to contribute to the improvement of the scientific basis for such risk assessments.

## References

- [1] Pedersen, P. Terndrup, May 1995, Collision and Grounding Mechanics, WEMT'95, Copenhagen.
- [2] Pedersen, P. Terndrup, 1994, Ship Grounding and Hull-Girder Strength, Marine Structures, vol. 7, pp. 1-29.
- [3] Pedersen, P. Terndrup and Simonsen, B. Cerup, 1995, Dynamics of Ships Running Aground, J. of Marine Science and Technology, Vol. 1, pp. 37-45.
- [4] Mei, C.C., Yeung, R.W. and Liu, K.-F., 1985, Lifting of a Large Object from a Porous Seabed, J. of Fluid Mechanics, Vol. 152, pp. 203-215.
- [5] Harremoes, P. Ovesen, Krebs & Jacobsen, Moust, 1980, *Loerebog i geoteknik* (in Danish), Vol. 2, Polyteknisk Forlag, 4th edition.
- [6] Biot, M.A., 1941, Theory of Three-Dimensional Consolidation, J. of Applied Physics, Vol. 12, pp. 155-164.
- [7] Biot, M.A., 1960, Mechanics of Deformation and Acoustic Propagation in Porous Media, J. of Applied Physics, Vol. 33, pp. 1483-1498.
- [8] Zienkiewicz, O.C., C.T. Chang and P. Bettles, 1980, Drained, Undrained, Consolidating, and Dynamic Behaviour Assumptions in Soils, Limits of Validity, Geotechnique, Vol. 30, pp.

- 385-395.
- [9] Englund, F., 1953, On the Laminar and Turbulent Flows of Ground Water through Homogeneous Sand, Trans. Dan. Acad. tec. Sc. Vol. 3.
  - [10] Sir Horrace Lamb, 1932, Hydordynamics, Cambridge University Press, 6th edition.
  - [11] Landweber, L. and Macagno, M., Mar. 1960, Added Mass of a Rigid Prolate Spheroid Oscillating Horizontally in a Free Surface, J. of Ship Research, pp. 30-36.
  - [12] Abkowitz.M.A., 1964, Lectures on Ship hydrodynamics - Steering and Manoeuverability, Report No. hy-5 Hydrodynamics Department, Danish maritime Institute.
  - [13] Ottesen Hansen, N.-E., Simonsen B.C. and Sterndorff, M.J., 1994, Soill Mecahnics of Ship Beaching, Proc. the 24th Int. Conf. on Coastal Engineering, Kobe.
  - [14] Sterndorff, M.J., Pedersen, P. Terndrup, 1996, Grounding Experiments on Soft Bottoms, J. of Marine Science and Technology, Vol. 1, pp. 174-181.
  - [15] B.C. Simonsen, The Mechanics of Ship Grounding, Ph.D.thesis, Department of Naval Architecture and offshore Engineering, Technical University of Denmark, Lyngby, Denmark
  - [16] B.C. Simonsen and P.T. Pedersen, 1998, On Grounding of Fast Ships, submitted for publication in Marine Structures.